Recrossings and Transition-State Theory

Huw O. Pritchard

Department of Chemistry, York University, Toronto, Canada M3J 1P3

Received: October 16, 2004; In Final Form: December 5, 2004

When classical trajectory calculations are run on the two isomerization reactions NCCN ⇌ NCNC and CH_3CN ⇌ CH_3NC over a long period of time, up to ca. 0.2 μs each, one finds many more recrossings than actual reactive events. In these calculations a "recrossing" is defined as passage over the potential barrier separating the two species followed by return to the original side within 0.2 ps. For the C_2N_2 case there are about twice as many crossings of the barrier as there are genuine reactive events, and for CH_3CN, there are about 10 times as many. Long-term mean residence times, τ^{∞}_{CN} and τ^{∞}_{NC}, in reactant and product wells are compared with the corresponding mean first passage times, τ^{1}_{CN} and τ^{1}_{NC}, the latter found by terminating the trajectories at the first crossing of the barrier. For the NCCN ⇌ NCNC reaction, except at the lowest energies, the mean residence times are exactly twice the mean first passage times, implying that the transition-state theory transmission coefficient, as traditionally defined, should be $\kappa = 0.5$.

Introduction

With continuing increases in computing power it has become possible to observe reactive trajectories by "ab initio molecular dynamics" calculations in which the energy and its gradients at a particular geometric arrangement are found by using standard ab initio procedures and the motion followed by classical trajectory methods. Surprisingly, unexpected numbers of recrossings of the potential barrier have been observed within the picosecond time scale for some simple isomerization reactions of vinylidene[1] and the cyclopropyl radical;[2] the former result was soon corroborated by a full quantum wave packet calculation.[3] Similar recrossings were observed in a calculation on the reaction $Cl^- + CH_3Cl \rightleftharpoons ClCH_3 + Cl^-$, but the integration times were insufficient for an estimate of the reaction rate to be compared with the transition-state value.[4]

Such results are mostly limited to the femtosecond time range or up to a few picoseconds, but many reactions of practical importance to which transition-state theory is applied take place on millisecond, second, or even longer time scales; it is therefore important to consider *much* longer computational time scales. On the other hand, traditional trajectory methods in which a potential-energy surface is constructed beforehand are readily extended to submicrosecond durations, enabling comparison with the results of conventional transition-state theory to be made.

In this paper we extend our earlier one-trip trajectory calculations on two simple isomerization reactions in order to examine their long-time crossing behavior: first, CH_3CN ⇌ CH_3NC using an interpolated potential surface constructed from known experimental and ab initio results[5] and NCCN ⇌ NCNC using an analytic four-body function created by least-squares fit[6] to a set of 597 ab initio MP2/6-31G* energy values.[7] Both methods of construction have their drawbacks: the former was alleged (on the basis of irreversible behavior restated in Table 1) to provide insufficient coupling between internal degrees of freedom (IVR) that could lead, indirectly, to a failure in microscopic reversibility between the forward and reverse CH_3CN ⇌ CH_3NC reactions,[8] and in the latter it is difficult to know with certainty whether there exist spurious valleys or basins in which the trajectory could loiter either in the vicinity of the saddle point, causing unwanted recrossings, or away from it, causing retardation the reaction in one or both directions. Moreover, the fitting of large numbers of energy values to a complex polynomial is not a trivial exercise.[9]

Computational Procedure

In previous works[8] trajectories starting from either side of the barrier were terminated as soon as the saddle point was crossed, and the present work was undertaken to find whether the mean first passage times so obtained would coincide with the mean residence times for a single trajectory that was continued indefinitely. The earlier unidirectional routines[8] were altered appropriately for this purpose.

For each trial value of the energy trajectories were commenced from the normal internuclear configuration with random momenta assigned to each degree of freedom; the study was restricted to the behavior of rotationless, $J = 0$, molecules. Integrations were performed, as before,[10] by using a fourth-order Runge−Kutta procedure with fifth-order Adams−Mouton predictor−corrector. Integration steps of 0.1 fs were used whence energy was conserved to within 1 part in 10^{12} at 10 ps for the CH_3CN ⇌ CH_3NC reaction[11] and 1 part in 10^7 for the NCCN ⇌ NCNC reaction; the difference arises from a difference in complexity of the potential-energy functions, 20 versus 90 terms in the two cases, and the consequent proliferation of the number of derivatives to be evaluated. At longer times, for the NCCN ⇌ NCNC reaction, energy conservation held to within 1 part in 10^6 and 10^5 at 100 ps and 1 ns, respectively.

Occasionally, at low energies the random assignment of momenta placed insufficient energy in the bending modes and a single crossing would fail to occur far beyond the mean expected first passage time for that energy; such trajectories were rejected in the analysis below. Also, to avoid any hidden bias from this source, each trajectory was terminated at 1 ns and a new one was started; this, in an approximate manner, mimics the randomization that would occur upon each collision at a pressure of about 100 Torr. It also helps to keep the rounding errors within reasonable bounds.

10.1021/jp045262s CCC: $30.25
Published on Web 01/27/2005

TABLE 1: Comparison of Mean First Passage Times for Isomerization of X−NC and of X−CN (where X = CH_3 or NC)

energy[a]/cm^{-1}	$\rho(E)_{NC}$ (per cm^{-1})	$\rho(E)_{CN}$ (per cm^{-1})	$\rho(E)_{CN}/\rho(E)_{NC}$	τ^1_{NC}/ps	τ^1_{CN}/ps	τ^1_{CN}/τ^1_{NC}
		$CH_3NC \rightleftharpoons CH_3CN$ (100 trajectories)				
25 019	9.6×10^4	7.0×10^5	7.3	203	107	0.53
33 085	9.8×10^5	4.7×10^6	4.8	55	30	0.55
41 150	6.7×10^6	2.4×10^7	3.6	16	7	0.44
		NCNC ⇌ NCCN (1000 trajectories)				
13 814	7.4×10^2	1.2×10^4	16.2	7.6	105.6	13.9
15 528	1.3×10^3	1.7×10^4	13.1	3.7	43.0	11.6
18 361	3.1×10^3	3.0×10^4	9.7	1.8	15.3	8.5
20 809	5.9×10^3	4.6×10^4	7.8	1.1	8.2	7.5
26 055	1.9×10^4	1.1×10^5	5.5	0.6	2.7	4.5

[a] For consistency with earlier papers,[7,8] energies listed in column 1 are for the isocyanide molecule, relative to the $v = 0$ level; those for the cyanide isomer are greater by 8256 and 11 084 cm^{-1} for CH_3CN and NCCN, respectively.

For the $CH_3CN \rightleftharpoons CH_3NC$ case, to amass a large number of crossings, it was necessary to use fairly high energy values[11a] at which C−H dissociation could occur. Typically, for the three energy values used, an average of 100, 80, and 30 crossings took place before dissociation occurred and the next trajectory in the ensemble was commenced.

The NCCN ⇌ NCNC case presents the additional complications that NCNC can also isomerize into CNNC and that there are two ways in which NCCN can change into NCNC; the former possibility was excluded by keeping the trial values of the energy below this threshold, and symmetry number considerations[12a] can be, in the main, avoided in the comparisons because they apply equally to the reaction of NCCN in both the one-trip and the extended calculations.

In addition, the existing potential-energy surface[7] was examined for defects, and it was found that there were two unwanted depressions, one at fairly large NC−CN separations and the other near the barrier to CNNC. These were remedied by the inclusion of about 50 new MP2/6-31G* points covering these two regions to make (with deletion of a handful of very high lying values) a set of 640 energies for fitting to a new analytic function. This produced, somewhat unexpectedly, a diminution in the unidirectional lifetimes of a factor of up to about 3 or 4 with respect to those found previously.[8] Then, to try to ensure proper behavior in the transition region, another 230 energy points around the barrier were added, making a total of 870 points upon which the final potential-energy surface was based. The difference in lifetimes derived from the two new potentials was inconsequential, suggesting that there are no unwanted trapping areas in the barrier region.

One other possible cause of spurious recrossings was examined and discounted: in these calculations the potential energies are evaluated using internal coordinates (in the NCCN case, for example, r_{ij}, $1 \le i, j \le 4$, $i \ne j$) which could lead to an uncertainty in orientation as three atoms pass through linearity or four atoms through planarity. (This could have accounted for the much greater frequency of recrossings found in the $CH_3CN \rightleftharpoons CH_3NC$ reaction since there are many more ways in which such coincidences could occur.) Long stretches of coordinates and momenta during clusters of recrossings (see Figure 2) were examined, but no sudden reversal of any component of momentum was ever detected.

Results

(a) $CH_3CN \rightleftharpoons CH_3NC$ Reaction. The occurrence of large numbers of recrossings on a very short time scale was noticed during the earlier investigation[8] but was deferred for later examination. Figure 1 depicts a histogram of the residence times in the CH_3NC well at an energy of 25 019 cm^{-1}. The distribution

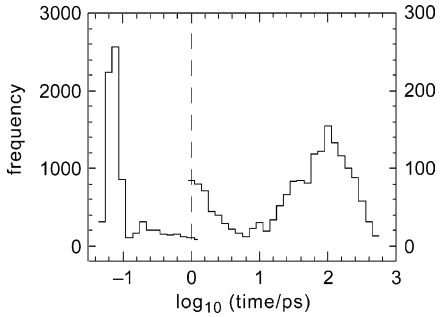

Figure 1. Distribution of residence times for transitions from CH_3NC to CH_3CN at an energy of 25 019 cm^{-1}. (Note the change in vertical scale at $t = 1$ ps).

is clearly bimodal with a large preponderance of crossings occurring before 1 ps and a smaller number of reactive events peaking around 100 ps. Figure 2 shows a typical 300 ps segment of a trajectory in which the central portion indicates upon which side of the barrier the system resides and the outer portions represent the potential energies at which the crossings occur; it is seen that the crossings tend to come in clusters, the feature near 200 ps lasting about 3.7 ps with a 0.48 ps gap partway through and containing 49 events in all. An obvious conclusion from this diagram is that within a cluster the crossings do not occur at the same potential-energy value, implying that significant redistribution of energy occurs on this time scale.

(b) NCCN ⇌ NCNC Reaction. The results for this reaction yield diagrams at all energies very like those shown in Figures 1 and 2, except that crossings come in smaller clusters, no more than 10−12 at a time. One example of a bimodal distribution is shown in Figure 3.

In every case the mean residence times in either well of the *recrossing trajectories* were within a few percent of 0.1 ps for both reaction systems. Figure 2 and the ones like it for this reaction suggest that this recrossing phenomenon is not caused by inefficient IVR, as suggested previously.[1] Crossing-point energies exhibit a sinusoidal distribution about the midpoint between the barrier and the total energy, as we noted earlier.[8] Exact coincidences between successive pairs of energy values for *nonreactive* crossings, printed out to four significant figures, were the same for both reactions, at about 0.05%, and recurrences to within ±0.1% and ±1% were, respectively, about 0.5% and 5%; given the sinusoidal distribution, these probabilities are close to being statistical.

Data Analysis

Table 1 shows the corrected data for the mean first passage times of the forward and reverse processes in both reactions. Despite the procedural changes noted above, the conclusions

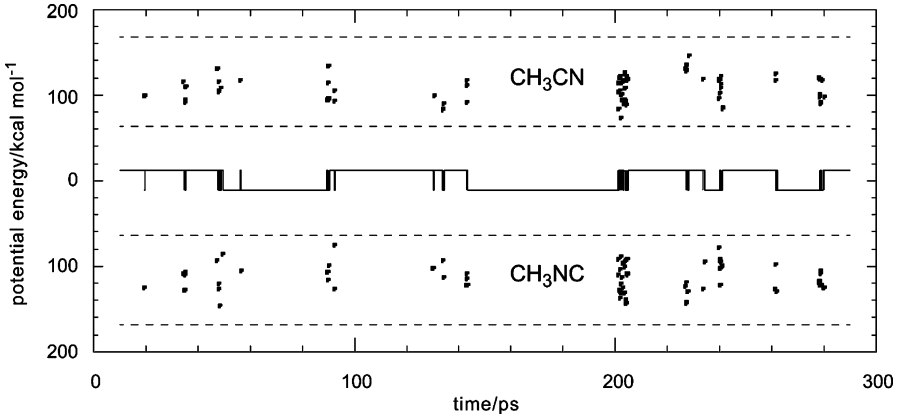

Figure 2. Distribution of crossing times and crossing energies for $CH_3CN \rightleftharpoons CH_3NC$ processes at a total energy of 41 150 cm^{-1}. The horizontal dashed lines represent either the barrier height or the maximum energy, measured from the minimum of the CH_3CN well. In the central portion of the diagram a horizontal segment above the zero line depicts residence in the CH_3CN well, likewise for CH_3NC when below.

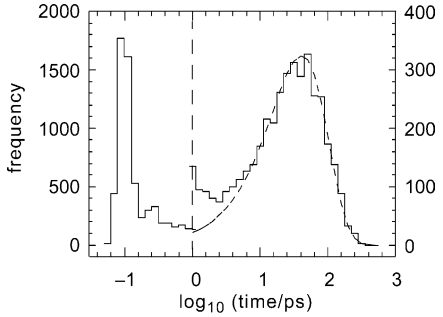

Figure 3. Distribution of residence times for transitions from NCCN to NCNC at an energy of 15 528 cm^{-1}. (Note the change in vertical scale at $t = 1$ ps).

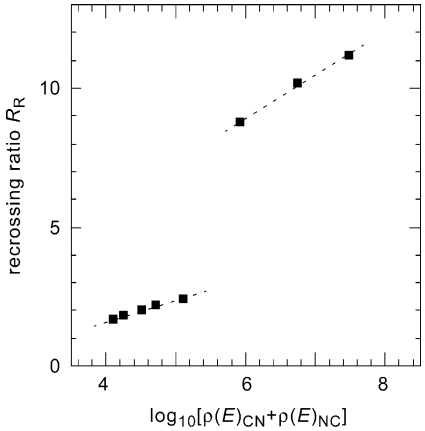

Figure 4. Recrossing ratios R_R versus densities of states ($\rho(E)_{CN} + \rho(E)_{NC}$) for the NCCN $\rightleftharpoons$ NCNC and $CH_3CN \rightleftharpoons CH_3NC$ reactions.

are as before:[8] that there is a gross failure to observe microscopic reversibility, i.e.

$$\rho(E)_{NC}/\tau^1_{NC} = \rho(E)_{CN}/\tau^1_{CN}$$

in the $CH_3CN \rightleftharpoons CH_3NC$ reaction where the interpolated analytic potential surface was used, whereas for the NCCN $\rightleftharpoons$ NCNC reaction, where an (improved) empirical potential surface was used, microscopic reversibility is fairly well obeyed, remembering that the densities of states are only simple harmonic oscillator approximations.

Table 2 gives the statistics from trajectories that were allowed to run beyond the first passage time for which the cumulative reaction time over all trajectories is a little over 1 μs. For the $CH_3CN \rightleftharpoons CH_3NC$ reaction the total numbers of crossings exceed the numbers of truly reactive crossings by an order of magnitude, whereas in the NCCN $\rightleftharpoons$ NCNC reaction the discrepancy is only about a factor of 2; in both cases, however, this recrossing ratio, R_R, increases with increasing energy and therefore densities of states, as shown in Figure 4. This is not an unexpected result; see, for example, refs 13 and 14.

Again, the pairs of residence times for the $CH_3CN \rightleftharpoons CH_3NC$ reaction do not obey microscopic reversibility, although here the mean lifetimes for isocyanide are shorter than for cyanide, as they should be, and not longer as they were in Table 1. The reason for these discrepancies, in both Tables 1 and 2, is not clear but may arise from some unsuspected discontinuities, perhaps in the handling of the switching functions used in the potential-energy formulation.[5] If so, this is a problem that may compromise other trajectory simulations that use similar kinds of potential functions, perhaps in protein folding, for example.

On the other hand, the situation is very satisfactory for the NCCN $\rightleftharpoons$ NCNC case as far as microscopic reversibility is concerned. However, the mean residence times in the two penultimate columns of the lower half of Table 2 are approximately a factor of 2 greater than the corresponding mean first passage times throughout Table 1; these differences are explained in more detail below. It should also be noted that the

TABLE 2: Recrossing Statistics for Extended Trajectories and Mean Residence Times Following Reactive Events

energy/cm^{-1}	cumulative time/ns	total crossings	reactive crossings	ratio R_R	τ^{∞}_{NC}/ps	τ^{∞}_{CN}/ps	$\tau^{\infty}_{CN}/\tau^{\infty}_{NC}$
			$CH_3NC \rightleftharpoons CH_3CN$				
25 019	243	19 425	2217	8.8	191.4	206.6	1.1
33 085	281	80 455	7918	10.2	56.4	76.0	1.3
41 150	248	168 961	15 142	11.2	18.8	31.6	1.7
			NCNC $\rightleftharpoons$ NCCN				
13 814	100	4605	2717	1.69	14.0	179.0	12.8
15 528	200	23 574	12 949	1.82	7.2	79.4	11.1
18 361	40	13 109	6499	2.02	3.6	31.0	8.8
20 809	20	12 172	5477	2.22	2.4	16.8	7.2
26 055	20	29 508	12 109	2.45	1.4	5.4	3.9

TABLE 3: Mean NCCN Lifetimes Adjusted for Recrossing Ratios

energy/cm^{-1}	R_R	τ^1_{CN}/ps	{min2|R_R}τ^1_{CN}/ps	τ^∞_{CN}/ps
13 814	1.69	105.6	178.5	179.0
15 528	1.82	43.0	78.3	79.4
18 361	2.02	15.3	30.6	31.0
20 809	2.22	8.2	16.4	16.8
26 055	2.45	2.7	5.4	5.4

division between recrossing and reaction, placed at 0.2 ps, is rather subjective, and a different choice would alter some of the *shorter* mean residence times by as much as 20−30%, whereas those longer than about 15 ps are negligibly affected.

Discussion

Due to the imperfections in the $CH_3CN \rightleftharpoons CH_3NC$ calculations already exposed, the remainder of this summary will concentrate mainly on the NCCN ⇌ NCNC results. The former are only of qualitative significance and included as evidence that the bimodal distributions found in Figures 1 and 3 probably represent a more general pattern and to call attention to some unresolved problems.

As mentioned, the mean residence times for NCNC are too short to be considered accurate, but we see that at the three highest energies the mean residence times for NCCN are virtually exactly twice those of the corresponding first passage times. It is clear that here we have a situation somewhat like that envisaged by Polanyi[15] and expanded upon later by many others[16,17a] wherein the potential-energy surface representing the reaction

$$H + H_2 \rightarrow H_2 + H$$

has a basin at the top of the barrier in which the trajectory may be trapped temporarily and from which it stands an equal chance of emerging in either the forward or the reverse direction. Thus, the transmission coefficient κ will then be one-half rather than unity, which it would be if there were no basin.[17b]

This is quite unlike the alternative models of Hirschfelder and Wigner[17c,18,19] and of Miller[20] in which the recrossings exhibit random gap behavior and the transmission coefficient can take *any* value $\kappa \leq 1$ depending upon the magnitudes of the reflection coefficients.

In the present case there is no depression at the barrier along the minimum energy path and no obvious signs of one in the vicinity. Animation of the trajectories within these clusters of recrossings reveals a complicated set of twisting and breathing motions in which the ends of the two CN groups continually exchange allegiance with either C atom having an equal chance of being terminal. There is no propensity for a return from the transition region to the original region of phase space, as found in some other trajectory calculations.[21]

At the two lowest energies Table 2 shows recrossing ratios $R_R < 2$, and therefore, the transmission coefficient κ must be greater than one-half: simply multiplying the mean first passage times τ^1_{CN} by {min2|R_R} yields numbers virtually identical with the corresponding mean residence times τ^∞_{CN}, as in Table 3. Perhaps we could associate these values of the recrossing ratio $R_R < 2$ with the onset of small-molecule unimolecular reaction behavior[11b] for which the transmission coefficient would then be R_R^{-1}.

The bimodal distribution of residence lifetimes exhibited in Figures 1 and 3 was unexpected: for the one-trip trajectories the distribution of lifetimes conforms to the usual unimolecular exponential decay pattern,[7,11b] but for the nonrecrossing trajectories it does not. The latter gives the appearance that escape from the NCCN well is a two-step process

$$A \xrightarrow{k_1} B \xrightarrow{k_2} C$$

The standard expression for the concentration [B] as a function of time is[12b]

$$[B] = [A]_0 k_1 (e^{-k_1 t} - e^{-k_2 t})/(k_2 - k_1) \quad (1)$$

$$\xrightarrow{k_2 \rightarrow k_1} [A]_0 k_1 t e^{-k_1 t} \quad (2)$$

The function that approximates the right-hand hump in Figure 3 has the same form, viz

$$N(\tau) = N_0 k_1 \tau e^{-k_1 \tau} \quad \text{or} \quad N(\tau) = N_0 \tau/\tau^\infty_{CN}\, e^{-\tau/\tau^\infty_{CN}} \quad (3)$$

with $k_1 = 1/\tau^\infty_{CN}$ and N_0, which depends on the total number of crossings, adjusted to fit. This is similar for the other NCCN lifetimes in Table 2 but somewhat more ambiguous for those of NCNC because the tail of the short-time recrossing peak merges significantly into the reaction peak.

It should be noted that the simple A ⇌ B isomerization reaction was extensively treated as a three-state process ca. 20 years ago,[22,23] but the distribution of lifetimes between the various domains was not discussed. Further reexamination in light of these new results is clearly warranted.

In an earlier numerical experiment on NCNC[7] we found mean first passage time distributions conforming to eq 1 when trajectories were started from a nonrandom distribution (zero kinetic energy) with k_2 being identical with $1/\tau^1_{NC}$ and k_1 interpreted as the rate constant for approach to the randomized state from which isomerization took place. In this light the equality of k_1 and k_2 that is implied in eq 3 becomes plausible: if each trajectory were to be run backward from its 1 ns end point (at infinite precision so that it did not diverge), then the same distribution of residence times would be found but with labels 1 and 2 interchanged. Moreover, the observation in Table 3 that $\tau^\infty_{CN} = 2\tau^1_{CN}$ is consistent with the fact that for the distribution function $P(t) = k_1 t \exp(-k_1 t)$ the mean lifetime $\bar{t} = 2/k_1$.

One can also match the CH_3CN and CH_3NC peaks to similar functions but only with $k_1 \neq k_2$, possibly related to the shortcomings of those trajectory results already mentioned.

In addition to a fundamental understanding of the reasons for the occurrence of the distribution function eq 3, with the possible implication that return from the transition region resembles emergence from an ordered state, some other questions remain to be answered. It is not clear what determines the recrossing ratio, R_R, other than that, as shown in Figure 4, it increases with density of states, i.e., either with increasing energy or with increasing molecular complexity, nor whether the large step in R_R arises from these effects or from an insufficiency of coupling between the vibrational modes which we have alleged on previous occasions[7,8] to impede proper randomization in the $CH_3CN \rightleftharpoons CH_3NC$ case. These are important questions since, in the absence of tunneling, the transmission coefficient is given by

$$\kappa = \{\text{min2}|R_R\}^{-1} \quad (4)$$

Recently, Truhlar and co-workers[24] redefined the transmission coefficient to include the augmentation of the rate by tunneling as well as retardation from causes noted above. This is perhaps unfortunate at the present juncture as the former is a quantum

process that can occur at any energy (but has its greatest import below the classical barrier) and the latter are classical manifestations which occur solely at or above the classical barrier. However, in a fully quantum (wave packet)[3] calculation such a distinction would disappear. Nevertheless, there is an interesting confluence in behavior on both sides of the barrier, with the possibility that a unifying concept can be achieved through an appeal to Ehrenfest's theorem. The approximate convergence of classical and quantal descriptions with increasing energy or density of states is well known.[25,26] It is most simply shown for a single harmonic oscillator as the approach of the quantal solution toward the classical one[25b,26] or for a single Morse oscillator[27] and is equally applicable to any collection of anharmonic oscillators. The present results show, conversely, an approach of the classical result toward the quantum picture: when the molecule finds itself in the immediate vicinity of the transition region, it stands an equal chance of going either to product or back to reactant. The corresponding behavior is very familiar in the tunneling region, where the transmission coefficient approaches one-half as the width of the (symmetric) barrier approaches zero[28,29] only here we have an infinitesimally thin multidimensional sheet dividing the reactants from the products. A possible framework for examining this correspondence could involve further development of the Feynman path integral formulation.[30]

Conclusions

Given a properly constructed potential-energy surface for a unimolecular isomerization reaction (and at high energies for small molecules or at all energies for larger molecules), the principal conclusions from this experiment are that (1) the mean residence times in the reactant and product wells should be exactly twice the corresponding mean first passage times for the forward and reverse reactions and (2) pairs of lifetimes obey the required condition of microscopic reversibility.

Conclusion 1 arises from the fact that in such reaction systems there are many more crossings and recrossings of the transition barrier than there are truly reactive events: when crossings occur, they tend to come in tight clusters, giving the coarse-grained appearance of either a successful or a failed reactive event, with approximately equal probability. Also, Figure 2 (and others like it for both reaction systems) shows these recrossings are not the result of ineffective randomization of internal energy.

Assuming that the NCCN $\rightleftharpoons$ NCNC reaction lies approximately on the border between small- and large-molecule behavior, we can expect that in most unimolecular reactions there will always be at least twice as many crossings and recrossings as there are reactive events, and such recrossings can come in clusters of as many as 10 or 20 at a time.

Because these recrossings occur in short clusters with relatively long time intervals between them, the maximum possible value of the transmission coefficient for the unimolecular transformation of a large molecule, in the absence of tunneling, will be $\kappa = 1/2$. Consequently, strict adherence to transition-state theory, in the sense that $\kappa = 1$,[13,14] can only occur in the small-molecule limit and possibly likewise for bimolecular atom transfer reactions.

At this time these conclusions are claimed only for the two isomerization reactions described in this paper and maybe for the isomerization[1−3] and exchange[4] reactions mentioned earlier, all of them for isolated systems in vacuo; further work, both experimental and computational, will be needed to demarcate their generality.

Acknowledgment. I thank Dr. Raj Vatsya for discussions about Ehrenfest's theorem.

References and Notes

(1) Hayes, R. L.; Fattal, E.; Govind, N.; Carter, E. A. *J. Am. Chem. Soc.* **2001**, *123*, 641−657.
(2) Mann, D. J.; Hase, W. L. *J. Am. Chem. Soc.* **2002**, *124*, 3208−3209.
(3) Schork, R.; Köppel, H. *J. Chem. Phys.* **2001**, *115*, 7907−7923.
(4) Sun, L.; Hase, W. L.; Song, K. *J. Am. Chem. Soc.* **2001**, *123*, 5753−5756.
(5) Sumpter, B. G.; Thompson, D. L. *J. Chem. Phys.* **1987**, *87*, 5809−5819.
(6) Press, W. H.; Flannery, B. P.; Teukolsky, S. A.; Vetterling, W. T. *Numerical Recipes: The Art of Scientific Computing*; Cambridge University Press: Cambridge, 1985.
(7) Shen, D.; Pritchard, H. O. *J. Chem. Soc., Faraday Trans.* **1996**, *92*, 4357−4360.
(8) Pritchard, H. O.; Vatsya, S. R.; Shen, D. *J. Chem. Phys.* **1999**, *110*, 9384−9389.
(9) Miller, W. H. *Faraday Discuss.* **1998**, *110*, 1−21.
(10) Shen, D.; Pritchard, H. O. *J. Chem. Soc., Faraday Trans.* **1991**, *87*, 3595−3600.
(11) (a) Shen, D.; Pritchard, H. O. *J. Phys. Chem.* **1994**, *98*, 1743−1745. (b) Shen, D.; Pritchard, H. O. *Int. J. Chem. Kinet.* **1994**, *26*, 729−736.
(12) (a) Laidler, K. J. *Chemical Kinetics*, 3rd ed.; Harper & Row: New York, 1987; pp 98−106. (b) Laidler, K. J. *Chemical Kinetics*, 3rd ed.; Harper & Row: New York, 1987; p 280.
(13) Pechukas, P.; McLafferty, F. J. *J. Chem. Phys.* **1973**, *58*, 1622−1625.
(14) Miller, W. H. *J. Phys. Chem. A* **1998**, *102*, 793−806.
(15) Polanyi, M. *Atomic Reactions*; Williams and Norgate: London, 1932; pp 14−26.
(16) Hirschfelder, J. O.; Eyring, H.; Topley, B. *J. Chem. Phys.* **1936**, *4*, 170−177.
(17) (a) Glasstone, S.; Laidler, K. J.; Eyring, H. *The Theory of Rate Processes*; McGraw-Hill: New York, 1941; pp 107−112. (b) Glasstone, S.; Laidler, K. J.; Eyring, H. *The Theory of Rate Processes*; McGraw-Hill: New York, 1941; pp 207−208. (c) Glasstone, S.; Laidler, K. J.; Eyring, H. *The Theory of Rate Processes*; McGraw-Hill: New York, 1941; pp 146−148.
(18) Hirschfelder, J. O.; Wigner, E. *J. Chem. Phys.* **1939**, *7*, 616−628.
(19) Eyring, H.; Walter, J.; Kimball, G. E. *Quantum Chemistry*; Wiley: New York, 1944; pp 299−326.
(20) Miller, W. H. *J. Chem. Phys.* **1976**, *65*, 2216−2223.
(21) Miller, J. A.; Garrett, B. C. *Int. J. Chem. Kinet.* **1997**, *29*, 275−287.
(22) DeLeon, N.; Berne, B. J. *J. Chem. Phys.* **1981**, *75*, 3495−3510.
(23) Gray, S. K.; Rice, S. A. *J. Chem. Phys.* **1987**, *86*, 2020−2035.
(24) Truhlar, D. G.; Gao, J.; Alhambra, C.; Garcia-Viloca, M.; Corchado, J.; Sánchez, M. L.; Villà, J. *Acc. Chem. Res.* **2002**, *35*, 341−349.
(25) (a) Schiff, L. I. *Quantum Mechanics*, 2nd ed.; McGraw-Hill: London, 1955; pp 25−27. (b) Schiff, L. I. *Quantum Mechanics*, 2nd ed.; McGraw-Hill: London, 1955; pp 65−67.
(26) Pauling, L.; Wilson, E. B. *Introduction to Quantum Mechanics*; McGraw-Hill: New York, 1935; pp 73−77.
(27) Pritchard, H. O. *J. Phys. Chem.* **1961**, *65*, 504−510 (Figure 1).
(28) Kemble, E. C. *The Fundamental Principles of Quantum Mechanics*; Dover: New York, 1937; p 111.
(29) Chan, W.-T.; Heck, S. M.; Pritchard, H. O. *Phys. Chem. Chem. Phys.* **2001**, *3*, 56−62 (Table A5).
(30) Vatsya, S. R.; Pritchard, H. O. Connection between classical and quantum descriptions of evolution. In *Causality and Locality in Modern Physics*; Kluwer: Dordrecht, 1998; pp 441−450.